ELSEVIER

Biophysical Chemistry 110 (2004) 203–211

Biophysical Chemistry

www.elsevier.com/locate/bpc

pH-dependent conformational changes of ferricytochrome *c* induced by electrode surface microstructure

Xiue Jiang, Xiaohu Qu, Lei Zhang, Zheling Zhang, Junguang Jiang, Erkang Wang, Shaojun Dong*

State Key Laboratory of Electroanalytical Chemistry, Changchun Institute of Applied Chemistry, Chinese Academy of Sciences, Changchun, Jilin 130022, China

Received in revised form 14 January 2004; accepted 17 February 2004
Available online 27 April 2004

Abstract

pH-dependent processes of bovine heart ferricytochrome *c* have been investigated by electronic absorption and circular dichroism (CD) spectra at functionalized single-wall carbon nanotubes (SWNTs) modified glass carbon electrode (SWNTs/GCE) using a long optical path thin layer cell. These methods enabled the pH-dependent conformational changes arising from the heme structure change to be monitored. The spectra obtained at functionalized SWNTs/GCE reflect electrode surface microstructure-dependent changes for pH-induced protein conformation, pK_a of alkaline transition and structural microenvironment of the ferricytochrome *c* heme. pH-dependent conformational distribution curves of ferricytochrome *c* obtained by analysis of in situ CD spectra using singular value decomposition least square (SVDLS) method show that the functionalized SWNTs can retain native conformational stability of ferricytochrome *c* during alkaline transition.

Keywords: CD spectra; SWNTs modified electrode; Electrode surface microstructure; Alkaline conformational changes of ferricytochrome *c*

1. Introduction

The influence of pH on electronic absorption spectra of ferricytochrome *c* has been focused for many years. One of the main reasons is that ferricytochrome *c* serves as an excellent model for studying conformational diversities of pH-dependent protein [1–6] and structure disturbance induced by binding other electron-transfer proteins [7]. Usually, ferricytochrome *c* undergoes a series of reversible conformational transitions accompanying the substitution of axial methionine ligand (Met 80) of the heme iron [8–10] in the range of pH 7–12. Among them, the "alkaline transition" leading from state III (cytochrome *c* at pH 7, His–Met act as axial ligands of heme iron) to the alkaline form state IV is one process that has been most thoroughly studied by many methods [8,11–15]; however, none of the experiments can give unambiguous explanation about the structural changes involved up to now.

Single- and multiwall carbon nanotubes (SWNTs and MWNTs) have drawn much attention in electrochemistry recently, and the direct electrochemistry of

* Corresponding author. Fax: +86-431-5689711.
E-mail address: dongsj@ns.ciac.jl.cn (S. Dong).

0301-4622/$ - see front matter © 2004 Elsevier B.V. All rights reserved.
doi:10.1016/j.bpc.2004.02.004

cytochrome *c* at MWNTs or SWNTs modified electrodes has been reported [16,17]. The results indicate that carbon nanotubes can accelerate the electron transfer between electrode and cytochrome *c*, and probably could retain the native conformation of cytochrome *c*. However, all these electrochemical experiments can only give macroscopic information and no further investigations, such as spectroscopic studies, have been reported about how the carbon nanotubes affect the conformational changes of cytochrome *c* in neutral or alkaline environment. However, a detailed understanding of the interaction mechanism between carbon nanotubes and cytochrome *c* can provide the essential information for optimization of conditions in this biosensor.

In the present report, CD, a powerful tool for studying the conformation of solution samples [18], and UV–vis spectroscopic techniques were used to investigate the pH-induced conformational changes of ferricytochrome *c* at functionalized SWNTs/GCE. Our main aim is to probe whether and how the functionalized SWNTs/GCE affect the secondary and tertiary conformational changes of ferricytochrome *c* during the pH variation. The experimental results show that the native conformation of ferricytochrome *c* can be protected at the functionalized SWNTs/GCE during pH variation to alkaline. The stabilizing mechanism and pH-induced conformational changes of ferricytochrome *c* at the functionalized SWNTs modified GCE have been discussed in terms of the effect of electrode surface microstructure.

2. Experiment

2.1. Materials and methods

Bovine heart cytochrome *c*, purchased from Sigma, was prepared in 0.1 M phosphate buffer solution (PBS). The concentration of solution was determined spectrophotometrically using a molar absorptivity of 1.06×10^5 mol^{-1} cm^{-1} at 410 nm for ferricytochrome *c* [19]. Phosphate buffer solutions used in all experiments were prepared by $Na_2HPO_4{\cdot}12H_2O$, $NaH_2PO_4{\cdot}2H_2O$ and Na_3PO_4 (analytical grade), doubly purified water was from Milli-Q system. The SWNTs (Shenzhen Nanotech Port) was pretreated through a well-established way with slight modification [20]. SWNTs (50 mg) were mixed with 100 ml 2.6 M HNO_3, refluxed at 120 °C for 24 h. Then diluted with water and filtered with 0.2 μm cellulose nitrate filtrate membrane (Gelman) under vacuum. The solid SWNTs were obtained by washing the remains on the filter with water until the filtrate pH became nearly neutral. Most of the catalyst particles were removed in this procedure. The paper-like SWNTs collected were further cut into short tubes by ultrasonicating in a 3:1 mixture of concentrated sulfuric and nitric acids (98% and 70%, respectively) for 8 h. The resultant suspension was then diluted with water, and the larger cut SWNTs were collected on a 0.2 μm membrane filter. After washed with 10 mM KOH and water, the purified and shortened SWNTs were collected. After the pretreatment, the SWNTs contain abundant oxygen-contained functionalities, such as carboxylic acid (–COOH) and hydroxyl (–OH) groups.

2.2. Instruments and methods

Spectroscopic experiments were carried out in a home-made long optical path thin layer cell (LOPTLC), AVIV 62A DS circular dichroism spectrometer (AVIV, USA) for CD spectrum measurement, Cary 500 UV–vis–NIR spectrometer (Varian, USA) for UV–visible spectrum measurement and a CHI 630 electrochemical instrument (CHI, USA) for electrochemical operation. The pretreated SWNTs modified glassy carbon (8×8 mm) electrode prepared according to literature [16] was used as working electrode, a twisted platinum wire as auxiliary electrode, and a Ag/AgCl (saturated KCl) as reference electrode. Before modification, the GCE was mechanically polished with 1.0, 0.3, and 0.05 μm α-Al_2O_3 slurry, successively, and then washed ultrasonically in water followed by ethanol for a few minutes at each step. The LOPTLC is of 10.0 mm optical path length and 0.2 mm thickness of thin layer. The incident light passed through the thin layer being parallel to the working electrode, so that the biomolecules on the electrode surface and in the solution could be monitored during the experiments. Before each measurement of pH-dependent CD or UV–visible spectrum, the electrolysis potential of LOPTLC was applied at 0.6 V for 5 min to keep all the cytochrome *c* molecules in their

oxidation state and interact with electrode surface completely.

2.3. Data analysis

To ascertain the different forms of ferricytochrome *c* presented over a range of solution pH, the CD spectral data were evaluated by Singular Value Decomposition Least Squares (SVDLS) analysis. In this analysis, several CD spectra were measured with the same *m* (*m*=total wavelengths) wavelengths. The spectra were grouped into series taken under identical conditions except for the changes of a single variable (as the pH). The SVDLS mathematical and computational details have been reported previously [21,22].

3. Results and discussion

3.1. Electronic absorption spectroscopy study

Ferricytochrome *c* at neutral state (state III) contains the His, Met-ligated form of the heme. The axial ligation of the methionine sulfur to heme iron in ferricytochrome *c* has moderate affinity. So this residue is susceptible to be substituted by another strong-field ligand [10,23]. This transition leads to the "alkaline" isomer (state VI). The characterization of ferricytochrome *c* transition from the neutral state (state III) to alkaline state (state IV) is experimentally very simple by using absorption spectroscopy. This alkaline transition causes the elimination of the absorption band at 695 nm and a shift in most of the major absorption bands, such as Soret band [24,25]. The apparent pK_a of alkaline transition is about 8.9–9.3 for free ferricytochrome *c* [11–15].

Fig. 1A shows the electronic absorption spectra of ferricytochrome *c* at 695 nm at bare (curve 1), native SWNTs (curve 2), and pretreated SWNTs (curve 3) modified GCE in alkaline solutions. It can be clearly seen that the absorbance band of ferricytochrome *c* at 695 nm almost disappears at GCE at pH 10.11, and a slight increase of the absorbance is observed at the unpretreated SWNTs modified GCE. Whereas, the pretreated SWNTs modified GCE still leads to a well-defined absor-

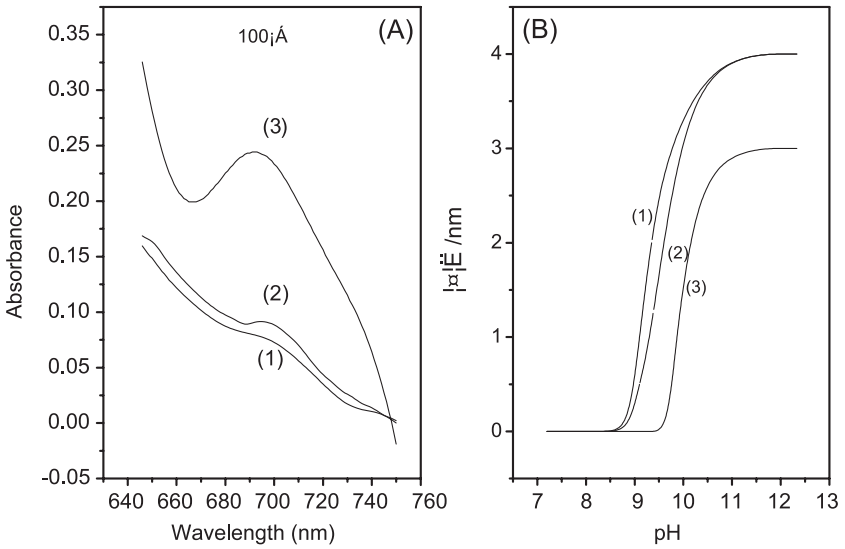

Fig. 1. (A) Electronic absorption spectra of ferricytochrome *c* at bare (curve 1), native SWNTs (curve 2), and functionalized SWNTs modified GCE (curve 3) in alkaline buffer solution; (B) plot of the difference between the maximal absorption wavelength of ferricytochrome *c* at pH 7.20 and those at higher pH values versus pH at bare (curve 1), native SWNTs (curve 2), and functionalized SWNTs modified GCE (curve 3). The pH values are 7.20, 8.43, 8.87, 9.10, 9.33, 9.67, 9.86, 10.11, 10.63, and 12.45, respectively.

bance peak at 695 nm at pH 10.63. Fig. 1B shows plot of the differences between the maximal absorption wavelength of ferricytochrome *c* at pH 7.20 and those at higher pH values ($\Delta\lambda$) versus pH at bare (curve 1), native SWNTs (curve 2), and pretreated SWNTs (curve 3) modified GCE in alkaline solutions. Based on the inflexion of curve 1, the pK_a of 9.3 for ferricytochrome *c* at bare GCE can be estimated, which is the same as that previously reported about the free ferricytochrome *c* during pH change to alkaline [11–15]. Similarly, the pK_a value of 9.5 can be obtained at native SWNTs modified electrode, indicating a little influence of the unpretreated SWNTs to ferricytochrome *c*. Whereas, the pretreated SWNTs modified GCE results in obvious increase of pK_a of ferricytochrome *c* to 10.2. These results indicate that functionalized SWNTs can protect the stability of ferricytochrome *c* native state (state III) at higher pH.

The changes for ferricytochrome *c* resulted from the effect of functionalized SWNTs have the similar manner to those observed for a complex formed by cytochrome *c* and cytochrome *c* oxidase [26] or other polyanions [26,27]. This indicates that the functionalized SWNTs can stabilize the disruption of Met 80–Fe bond as those complexes. The loss of Met 80 is triggered by the deprotonation of heme internal group [8,28,29], then the Met 80 ligand is removed physically and a protein surface residue is brought in to replace it [29]. In order to deprotonate an internal group, a structure gating reaction is required to allow some solvent base to enter the protein interior to act as proton acceptor [29]. And in order to physically remove Met 80 from the heme and replace it with one of the surface residues, some gating structures, such as the Ω loop (residues 71–85), would be significant distorted [29]. So the opening degree of some gating structures would affect the disruption of Met 80–Fe bond, and subsequently affect the alkaline transition of ferricytochrome *c*. According to this theory, the gating structure of ferricytochrome *c* may be affected by the functionalized SWNTs, thus, the pH-dependent conformational changes of ferricytochrome *c* should also be affected by functionalized SWNTs. The detailed effect of functionalized SWNTs on ferricytochrome *c* conformation can be seen clearly in the following section.

3.2. Structure changes of ferricytochrome c in pH-induced reaction

3.2.1. Effect of electrode surface microstructure on pH-dependent conformational transitions of ferricytochrome c

Ferricytochrome *c* (4.7 μM) in 0.1 M PBS in a LOPTLC at bare GCE was used for CD spectroscopic measurement in far-UV region. The CD spectra in far-UV region provide information about the conformation of the polypeptide backbone [30]. Fig. 2A shows the pH-linked CD spectra of 4.7 μM ferricytochrome *c* in 0.1 M PBS solution at bare GCE. As can be seen from Fig. 2A, the negative cotton peaks decrease gradually with increasing of solution pH from 7.20 to 12.45. Fig. 2B and C shows the spectra of three pH-dependent conformations of ferricytochrome *c* obtained from Fig. 2A by SVDLS analysis and the corresponding pH-dependent plot of fractional distribution of the three conformations, respectively. It can be seen from Fig. 2B that only three conformations are changed with pH variation. According to Gauss–Markoff mode of protein secondary structure CD spectra and comparing with the CD spectra of 27 membrane proteins, curves (a), (b), and (c) are attributed to antiparallel β-sheet, α-helix, and α_T-helix, respectively [31,32]. α_T-helix is a denatured helical structure which is constituted by random coil and α-helix. As shown in Fig. 2C, the three conformations of antiparallel β-sheet, α-helix, and α_T-helix coexist in the solution at pH 7.20 with the fractions of 0.34, 0.61, and 0.05, respectively. When pH value increases to 9.50, the fraction of α_T-helix remains almost unchanged, while the fraction of α-helix decreases rapidly to 0.10, and the fraction of antiparallel β-sheet increases to 0.79. This implies that the conformational transition is mainly from α-helix to antiparallel β-sheet. The decrease of α-helix and the increase of antiparallel β-sheet indicate that the conformation of ferricytochrome *c* becomes incompact. With the increasing of pH from 9.50 to 12.45, the disruption of Met 80–Fe bond occurs, resulting in dramatically increase of α_T-helix fraction to 0.50 and decreases of antiparallel β-sheet and α-helix to 0.48 and 0.02, respectively. This indicates that the displacement of Met 80 by another strong-field ligand induces a more incompact conformational change.

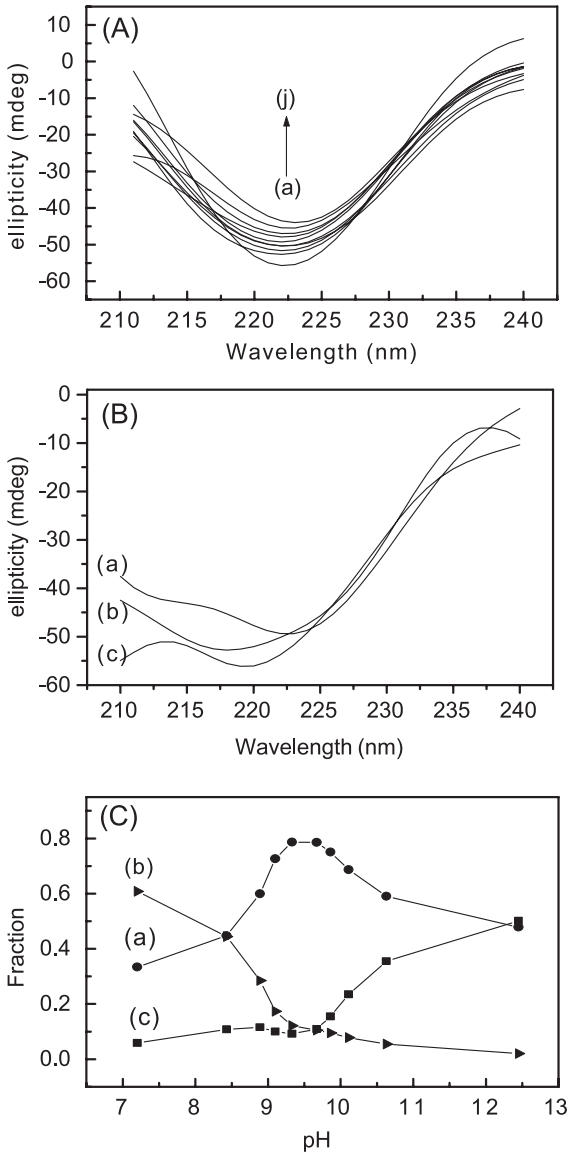

Fig. 2. (A) pH-linked CD spectra of 4.7 μM ferricytochrome *c* in 0.1 M PBS solution at GCE in a LOPTLC, pH values from (a) to (j) are: 7.20, 8.43, 8.87, 9.10, 9.33, 9.67, 9.86, 10.11, 10.63, and 12.45, respectively; (B) spectra of three pH-dependent conformations of ferricytochrome *c* obtained from Fig. 2(A) by SVDLS analysis; (C) the corresponding pH-dependent plot of fractional distribution of the three conformations. (a)–(c): Antiparallel β-sheet, α-helix, and α_T-helix.

Fig. 3 shows the far-UV pH-linked CD spectra of ferricytochrome *c* (Fig. 3A), the spectra of three pH-dependent conformations of ferricytochrome *c* (Fig. 3B) obtained from Fig. 3A by SVDLS analysis and the corresponding pH-dependent plot of fractional distribution of the three conformations (Fig. 3C) at

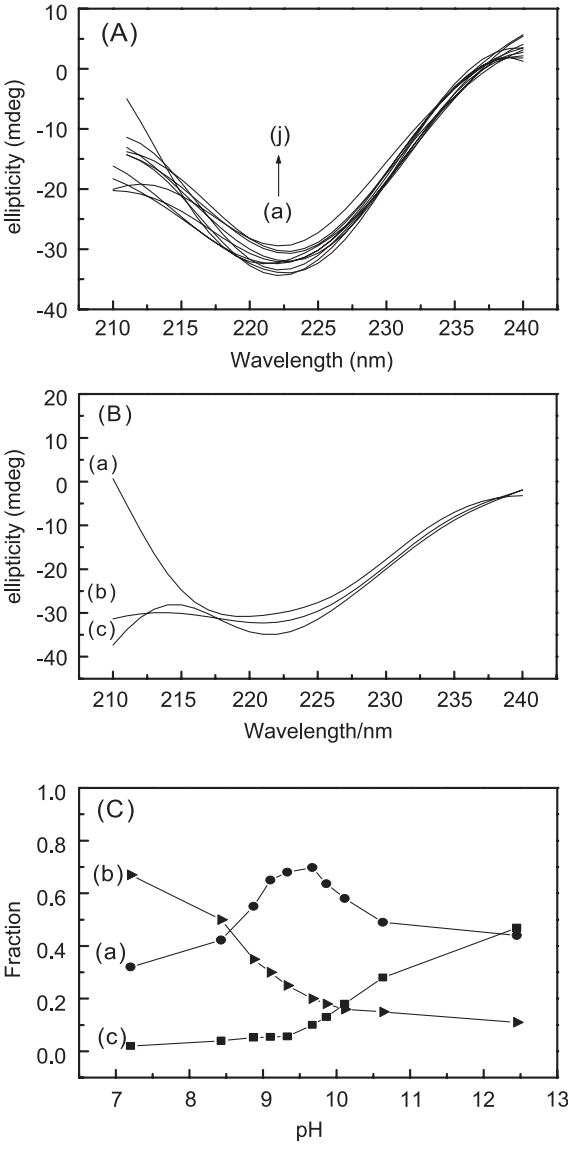

Fig. 3. (A) pH-linked CD spectra of 3.0 μM ferricytochrome *c* in 0.1 M PBS solution at unpretreated SWNTs modified GCE in a LOPTLC, pH values from (a) to (j) are: 7.20, 8.43, 8.87, 9.10, 9.33, 9.67, 9.86, 10.11, 10.63, and 12.45, respectively; (B) spectra of three pH-dependent conformations of ferricytochrome *c* obtained from Fig. 2A by SVDLS analysis; (C) the corresponding pH-dependent plot of fractional distribution of the three conformations. (a)–(c): Antiparallel β-sheet, α-helix, and α_T-helix.

the unpretreated SWNTs modified GCE. Compared with those in Fig. 2, there is no obvious difference between the responses of ferricytochrome *c* at bare and unpretreated SWNTs modified GCE. Whereas, it can be seen from Fig. 4A, the pH-linked CD spectra of ferricytochrome *c* at the pretreated SWNTs modified GCE, that the negative Cotton peaks increase gradually with increasing of pH from 7.20 to 12.45. This indicates that the conformational changes of ferricytochrome *c* are influenced strongly by pretreated SWNTs modified GCE surfaces. Fig. 4B shows the spectra of three pH-dependent conformations of ferricytochrome *c* obtained from Fig. 4A by SVDLS analysis. It can be seen from Fig. 4B that three conformations of α-helix (curve a), random coil (curve b), and parallel β-sheet (curve c) are changed due to the variation of pH. Fig. 4C shows the corresponding pH-dependent plot of fractional distribution of the three conformations shown in Fig. 4B. Compared with those in Figs. 2C and 3C, the three conformations of α-helix, parallel β-sheet, and random coil coexist with different fractions of 0.76, 0.09, and 0.14, respectively, in pH 7.20 PBS, and the fractions of all kinds of conformations have different changes when pH increases to 9.85. Especially in the case of α-helical fraction, there is dramatic decrease at bare and native SWNTs modified GCE whereas decreases only to 0.45 at pretreated SWNTs/GCE. This sufficiently proves that functionalized SWNTs do affect the conformational changes of ferricytochrome *c* in alkaline buffer solution, and, also, implies that the conformation is tighter at functionalized SWNTs/GCE than those at bare and native SWNTs modified GCE during pH variation to alkaline range, which fully supports our above suppose of "the gating structure of ferricytochrome *c* may be affected by the functionalized SWNTs". It is just this tighter conformation, which is not in favoring of the entry of solvent species into protein core to act as a proton acceptor, that improves the pK_a during alkaline transition. When pH continually increases from 9.85 to 12.45, the fractions of α-helical and random coil remain almost unchanged with the values of 0.43 and 0.17, respectively, whereas the fraction of parallel β-sheet increases to 0.40. This sufficiently indicates that the functionalized SWNTs can hold the conformation of ferricytochrome *c* during pH transition and

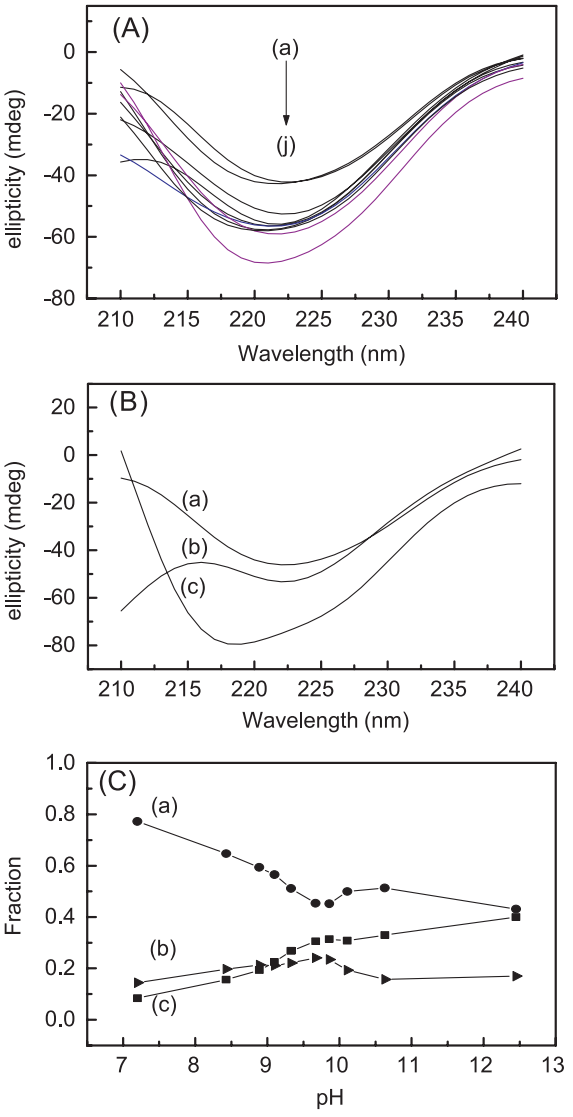

Fig. 4. (A) pH-linked CD spectra of 3.6 μM ferricytochrome *c* in 0.1 M PBS solution at pretreated SWNTs/GCE in a LOPTLC, pH values from (a) to (j) are: 7.20, 8.43, 8.87, 9.10, 9.33, 9.67, 9.86, 10.11, 10.63, and 12.45, respectively; (B) CD spectra of ferricytochrome *c* obtained by SVDLS analysis: (a) α-helix, (b) random coil, (c) parallel β-sheet; (C) pH-dependent conformations distribution curves of ferricytochrome *c* obtained by SVDLS analysis, (a)–(c): α-helix, random coil, and parallel β-sheet.

no large loss of α-helical fraction is caused even when the substitution of Met 80 by Lys ligand occurs. The main reason for the different conformational changes at different electrode surfaces during

pH variation to alkaline range may be interpreted in terms of the stabilization of ferricytochrome *c* structure arising from the specific interactions between protein and the promoter immobilized on the electrode surface [33]. This indicates that the electrode surface microstructure do affect the pH-induced conformational changes of ferricytochrome *c*. Antalik et al. [27] once reported that the presence of a negatively charged field created by covalently binding of polyanion was necessary for cytochrome *c* to form a structure with more stable Met 80–Fe bond. Moreover, Liu's group [34] also reported that the anion can screen the lysine and arginine surface charges, which reduces the lysine–lysine repulsions and suppresses the protein fluctuations. According to these results, the interactions between the negatively charged oxygen-containing groups on functionalized SWNTs surface and ferricytochrome *c* might provide a negatively charged field to screen the lysine and arginine surface charges, which makes the repulsions between lysine and lysine reduce. Thus, the conformation of ferricytochrome *c* becomes more stable.

3.2.2. The effect of electrode surface on pH-dependent tertiary structure changes in ferricytochrome c

The CD spectra in the Soret band can provide further insight into the environment of the heme [3]. The CD spectrum of ferricytochrome *c* obtained at bare GCE in 0.1 M PBS (pH 7.20) shows a positive Cotton peak at 400 nm and a negative Cotton peak at 418 nm (Fig. 5A). As can be seen from Fig. 5A, when solution pH increases to 12.45, the positive Cotton peak shows a red shift from 400 to 405 nm (curves (a)–(d)). As for the negative Cotton peak, a large decrease in intensity is caused when pH increases to 8.43 and disappears completely when solution pH is further increased to 10.11. This indicates that the structural microenvironment of the ferricytochrome *c* heme is changed accompanied with pH-induced conformational transitions. The red shift of the positive Cotton peak might be caused by the weakening of the axial ligand [35]. The negative band of CD spectrum at 418 nm in Soret region observed for ferricytochrome *c* is derived from the direct interaction of the π–π* transition of the aromatic ring of Phe-82 with the π–π* transition of heme group [35]. The disappearance of the negative Cotton peak might indicate that the distance and orientation of the Phe-82 residues positioned on the methionine side of the heme plane are changed [36].

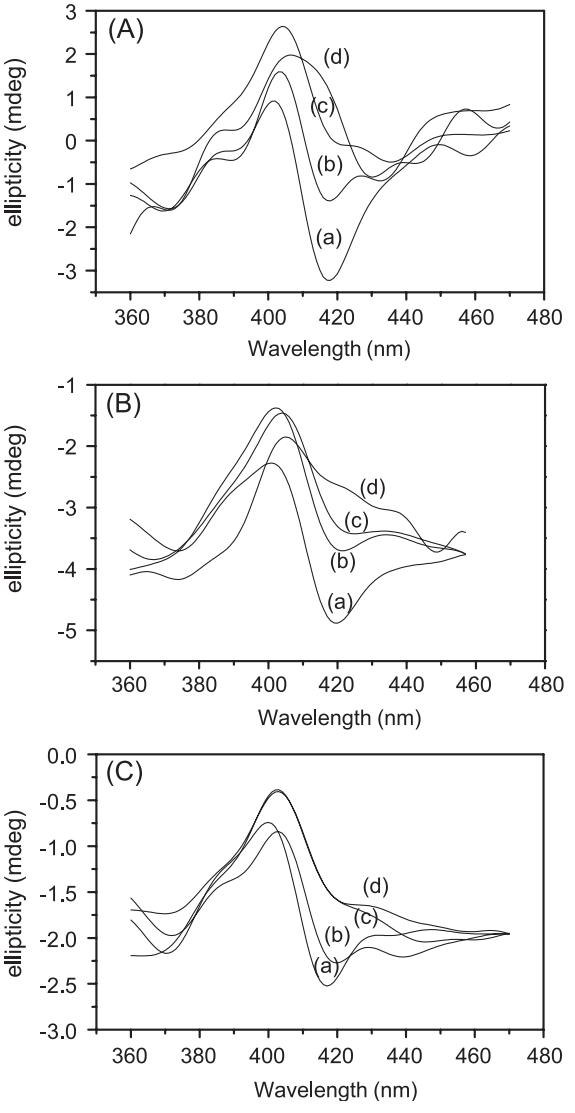

Fig. 5. pH-linked CD spectra of ferricytochrome *c* in Soret region in 0.1 M PBS in a LOPTLC at bare (A) and at the unpretreated SWNTs modified (B) GCE, pH: (a)–(d): 7.20, 8.43, 10.11, 12.45; (C) pH-linked CD spectra of ferricytochrome *c* in Soret region in 0.1 M PBS at pretreated SWNTs modified GCE in a LOPTLC. pH: (a)–(d): 7.20, 9.86, 10.63, 12.45.

Fig. 5B and C shows the pH-induced CD spectra of ferricytochrome *c* obtained at unpretreated and pretreated SWNTs modified GCE, respectively, in

0.1 M PBS. It can be seen from Fig. 5B that the influence of pH to the spectra of ferricytochrome *c* at the unpretreated SWNTs modified GCE is almost the same as that at bare GCE (Fig. 5A). Whereas, the pretreated SWNTs/GCE electrode leads to an obviously different changes of the spectra of ferricytochrome (Fig. 5C) compared with the spectra in Fig. 5A and B. Increasing of pH up to 12.45 only makes positive Cotton peak red shift to 402 nm (Fig. 5C, curve (d)). In addition, for the negative cotton peak, a small decrease is induced even when pH increases to 9.86 (Fig. 5C, curve (b)). The disappearance of the negative Cotton peak occurs when solution pH increases to 10.63 (Fig. 5C, curve (c)). All these differences indicate that the influence of functionalized SWNTs makes the pH-linked changes of structural microenvironment of the ferricytochrome *c* heme become more relaxation. Since the Soret CD of cytochrome *c* is the diagnostic for the Phe-82 state and the mobility of 75–87 residues loop will increase the distance between Phe-82 and the methionine side of the heme plane [37], thus, the mobility of the 75–87 residues loop will cause a drop in the strength of Phe-82–heme interaction and further result in the decrease of the negative Cotton peak. According to this conclusion, the different spectroscopic changes shown in Fig. 5 reflect that the functionalized SWNTs weaken the loops mobility and stabilize the rigid, native protein conformation. This also brings about different secondary conformational changes just as shown in the above experimental results.

Santucci et al. [37] have ascribed the weak of Met 80–Fe(III) bond caused by acid-denatured to the conditions employed. In neutral pH, the Met 80–Fe(III) bond is strengthened because the hydrogen bonds between loops decrease the loops mobility. In addition, in acidic environment, this condition cannot be satisfied because the high proton concentration will leave the protein with a high positive charge. As a result, the dynamic properties of the free loops are considerably enhanced. Thus, the axial bond might be weakened by the high degree of flexibility of the 70–85 residues loop. As for our experiments, the negatively charged field provided by functionalized SWNTs with $-COO^-$ groups may hinder the access of $-OH^-$ or other anions to loops in alkaline solution, so the hydrogen bonds between loops will not be affected, which will decrease the dynamic properties of free loops. This may be attributed to the protection of functionalized SWNTs to the disruption of Met 80–Fe(III) bond.

4. Conclusion

As a conclusion, the alkaline transition of ferricytochrome *c* and the effect of electrode surface microstructure on pH-induced conformational change were studied by CD and UV spectroscopy techniques. The results showed that the alkaline transition of ferricytochrome *c* accompanied with the different conformational changes at different electrode surfaces. The negatively charged field screen effect caused by interaction between negatively charged oxygen-containing groups on functionalized SWNTs surface and ferricytochrome *c* decreased the mobility of 70–85 residues loops and induced a more tight conformational change at SWNTs/GCE than that at GCE. This may be responsible for the different changes in pK_a during alkaline transition of ferricytochrome *c* due to the effect of electrode surface microstructure.

Acknowledgements

This work was supported by the National Natural Science Foundation of China (Nos. 20275037 and 20275036).

References

[1] J.M. Guss, P.R. Harrowell, M. Murata, V.A. Norris, Freeman H.C., Crystal structure analyses of reduced (Cu^I) polar plastocyanin at six pH values, J. Mol. Biol. 192 (1986) 361–387.
[2] T.F. Holzman, J.J. Dougherty, D.N. Brems, N.E. MacKenzie, pH-induced conformational states of bovine growth hormone, Biochemistry 29 (1990) 1255–1261.
[3] T. Takano, R.E. Dickerson, Conformation change of cytochrome *c*: I. Ferrocytochrome *c* structure refined at 1.5 Å resolution, J. Mol. Biol. 153 (1981) 79–94.
[4] G.V. Louie, G.D. Brayer, High-resolution refinement of yeast iso-1-cytochrome *c* and comparisons with other eukaryotic cytochrome *c*, J. Mol. Biol. 214 (1990) 527–555.
[5] G.W. Bushnell, G.V. Louie, G.D. Brayer, High resolution three-dimensional structure of horse heart cytochrome *c*, J. Mol. Biol. 214 (1990) 585–595.
[6] A.M. Berghuis, G.D. Brayer, Oxidation state-dependent con-

formational changes in cytochrome *c*, J. Mol. Biol. 223 (1992) 959–976.
[7] P. Hildebrandt, T. Heimburg, D. Marsh, G.L. Powell, Conformational changes in cytochrome *c* and cytochrome oxidase upon complex formation: a resonance Raman study, Biochemistry 29 (1990) 1661–1668.
[8] P.M.A. Gadsby, J. Peterson, N. Foote, C. Greenwood, A.J. Thomson, Identification of the ligand-exchange process in the alkaline transition of horse heart cytochrome *c*, Biochem. J. 246 (1987) 43–54.
[9] X. Hong, D.W. Dixon, NMR study of the alkaline isomerization of ferricytochrome *c*, FEBS 246 (1989) 105–108.
[10] J.C. Ferrer, J.G. Guillemette, R. Bogumil, S.C. Inglis, Smith M., A.G. Mauk, Identification of Lys79 as an iron ligand in one form of alkaline yeast iso-1-ferricytochrome *c*, J. Am. Chem. Soc. 115 (1993) 7507–7508.
[11] R.K. Gupta, S.H. Koenig, Some aspects of pH and temperature dependence of the NMR spectra of cytochrome *c*, Biochem. Biophys. Res. Commun. 45 (1971) 1134–1143.
[12] I. Morishima, S. Ogawa, T. Yonezawa, T. Iizuka, Nuclear magnetic resonance studies of hemoproteins: IX. pH dependent features of horse heart ferric cytochrome *c*, Biochim. Biophys. Acta 495 (1977) 287–298.
[13] H. Theorell, Å. Åkesson, Studies on cytochrome *c*: II. The optical properties of pure cytochrome *c* and some of its derivatives, J. Am. Chem. Soc. 63 (1941) 1812–1818.
[14] P. Tonge, G.R. Moore, C.W. Wharton, Fourier-transform infra-red studies of the alkaline isomerization of mitochondria cytochrome *c* and the ionization of carboxylic acids, Biochem. J. 258 (1989) 599–605.
[15] M. Assfalg, I. Bertini, A. Dolfi, P. Turano, A.G. Mauk, F.I. Rosell, H.B. Gray, Structure model for an alkaline form of ferricytochrome *c*, J. Am. Chem. Soc. 125 (2003) 2913–2922.
[16] J. Wang, M. Li, Z. Shi, N. Li, Z. Gu, Direct electrochemistry of cytochrome *c* at a glassy carbon electrode modified with single-wall carbon nanotubes, Anal. Chem. 74 (2002) 1993–1997.
[17] J.J. Davis, R.J. Coles, H.A.O. Hill, Protein electrochemistry at carbon nanotube electrodes, J. Electroanal. Chem. 440 (1997) 279–282.
[18] S.M. Kelly, N.C. Price, The application of circular dichroism to studies of protein folding and unfolding, Biochim. Biophys. Acta 1338 (1997) 161–185.
[19] J. Babul, E. Stellwagen, Participation of the protein ligands in the folding of cytochrome *c*, Biochemistry 11 (1972) 1195–1200.
[20] J. Liu, A.G. Rinzler, H. Dai, J.H. Hafner, R.K. Bradley, P.J. Boul, A. Lu, T. Iverson, K. Shelimov, C.B. Huffman, F.R. Macias, Y. Shon, T.R. Lee, D.T. Colbert, R.E. Smalley, Fullerence pipes, Science 280 (1998) 1253–1256.
[21] Y. Zhu, G. Cheng, S. Dong, Conformational transition of DNA in electroreduction studied by in situ UV and CD thin layer spectroelectrochemistry, Biophys. Chem. 87 (2000) 103–110.
[22] Y. Zhu, G. Cheng, S. Dong, The electrochemically induced conformational transition of disulfides in bovine serum albumin studied by thin layer circular dichroism spectroelectrochemistry, Biophy. Chem. 90 (2001) 1–8.
[23] S. Döpner, P. Hildebrandt, F.I. Rosell, A.G. Mauk, Alkaline conformational transitions of ferricytochrome *c* studied by Resonance Raman spectroscopy, J. Am. Chem. Soc. 120 (1998) 11246–11255.
[24] J. Bàgel'ová, Z. Gazová, E. Valušová, M. Antalik, Conformational stability of ferricytochrome *c* near the heme in its complex with heparin in alkaline pH, Carbohydr. Polym. 45 (2001) 227–232.
[25] F.I. Rosell, J.C. Ferrer, A.G. Mauk, Proton-linked protein conformational switching: definition of the alkaline conformational transition of yeast iso-1-ferricytochrome *c*, J. Am. Chem. Soc. 120 (1998) 11234–11245.
[26] M. Antalìk, M. Bona, J. Bágel'ová, Spectrophotometric detection of the interaction between cytochrome *c* and heparin, Biochem. Int. 28 (1992) 675–682.
[27] M. Antalìk, J. Bágel'ová, Z. Gazová, A. Musatov, D. Fedunová, Effect of varying polyglutamate chain length on the structure and stability of ferricytochrome *c*, Biochim. Biophys. Acta 1646 (2003) 11–20.
[28] G. Battistuzzi, M. Borsari, A. Ranieri, M. Sola, Effects of specific anion–protein binding on the alkaline transition of cytochrome *c*, Arch. Biochem. Biophys. 386 (2001) 117–122.
[29] L. Hoang, H. Maity, M.M.G. Krishna, Y. Lin, S.W. Engler, Folding units govern the cytochrome *c* alkaline transition, J. Mol. Biol. 331 (2003) 37–43.
[30] J.M. Scholtz, H. Qian, E.J. York, J.M. Stewart, R.L. Baldwin, Parameters of helix-coil transition theory for alanine-based peptides of varying chain lengths in water, Biopolymers 31 (1991) 1463–1470.
[31] R. Pribić, I.H.M. Vanstokkum, D. Chapman, P.I. Haris, M. Bloemendal, Protein secondary structure from Fourier Transform Infrared and/or Circular Dichroism Spectra, Anal. Biochem. 214 (1993) 366–378.
[32] J. Deisenhofer, O. Epp, K. Miki, R. Huber, H. Michel, Structure of the protein subunits in the photosynthetic reaction center of *Rhodopseudomonas viridis* at 3 Å resolution, Nature 318 (1985) 618–624.
[33] D.D. Schlereth, W. Maentele, Electrochemically induced conformational changes in cytochrome *c* monitored by Fourier Transform Infrared Difference Spectroscopy: influence of temperature, pH, and electrode surfaces, Biochemistry 32 (1993) 1118–1126.
[34] G. Liu, C.A. Grygon, T.G. Spiro, Ionic strength dependence of cytochrome *c* structure and Trp-59 H/D exchange from Ultraviolet Resonance Raman spectroscopy, Biochemistry 28 (1989) 5046–5050.
[35] C. Indiani, G. Sanctis, F. Neri, H. Santos, G. Smulevich, M. Coletta, Effect of pH on axial ligand coordination of cytochrome c^{11} from *Methylophilus methylotrophus* and horse heart cytochrome *c*, Biochemistry 39 (2000) 8234–8242.
[36] G.J. Pielak, K. Oikawa, A.G. Mauk, M. Smith, C.M. Kay, Elimination of the negative Soret cotton effect of cytochrome *c* by replacement of the invariant Phenylalanine using site-directed mutagenesis, J. Am. Chem. Soc. 108 (1986) 2724–2727.
[37] R. Santucci, C. Bongiovanni, G. Mei, T. Ferri, F. Polizio, A. Desideri, Anion size modulates the structure of the A State of cytochrome *c*, Biochemistry 39 (2000) 12632–12638.